East Asian Journal on Applied Mathematics
doi: 10.4208/eajam.200113.220213a

Vol. **3**, No. 1, pp. 59-80
February 2013

Stabilized Crank-Nicolson/Adams-Bashforth Schemes for Phase Field Models

Xinlong Feng[1,2], Tao Tang[1,*] and Jiang Yang[1]

[1] *Department of Mathematics & Institute for Computational and Theoretical Studies, Hong Kong Baptist University, Kowloon Tong, Hong Kong, China.*
[2] *College of Mathematics and System Sciences, Xinjiang University, Urumqi 830046, China.*

Received 20 January 2013; Accepted (in revised version) 22 February 2013

Available online 28 February 2013

Abstract. In this paper, stabilized Crank-Nicolson/Adams-Bashforth schemes are presented for the Allen-Cahn and Cahn-Hilliard equations. It is shown that the proposed time discretization schemes are either unconditionally energy stable, or conditionally energy stable under some reasonable stability conditions. Optimal error estimates for the semi-discrete schemes and fully-discrete schemes will be derived. Numerical experiments are carried out to demonstrate the theoretical results.

AMS subject classifications: 35L70, 65N30, 76D06

Key words: Allen-Cahn equation, Cahn-Hilliard equation, Crank-Nicolson scheme, Adams-Bashforth scheme, implicit-explicit method, error estimates.

1. Introduction

In this paper, we consider numerical approximations for the Allen-Cahn equation

$$\begin{cases} \dfrac{\partial u}{\partial t} = \Delta u - \dfrac{1}{\epsilon^2} f(u)\,, & (x,t) \in \Omega \times (0,T]\,, \\ \dfrac{\partial u}{\partial n} = 0\,, & (x,t) \in \partial\Omega \times (0,T]\,, \\ u|_{t=0} = u_0(x)\,, & x \in \Omega\,; \end{cases} \tag{1.1}$$

*Corresponding author. *Email addresses:* fxlmath@gmail.com (X. Feng), ttang@math.hkbu.edu.hk (T. Tang), jiangy@hkbu.edu.hk (J. Yang)

and the Cahn-Hilliard equation

$$\begin{cases} \dfrac{\partial u}{\partial t} = \Delta\left(-\Delta u + \dfrac{1}{\epsilon^2} f(u)\right), & (x,t) \in \Omega \times (0,T], \\ \dfrac{\partial u}{\partial n}|_{\partial\Omega} = 0, \quad \dfrac{\partial\left(\Delta u - \frac{1}{\epsilon} f(u)\right)}{\partial n} = 0, & (x,t) \in \partial\Omega \times (0,T], \\ u|_{t=0} = u_0(x), & x \in \Omega. \end{cases} \tag{1.2}$$

In the above equations, $u = u(x,t)$ represents the concentration of one of the two metallic components of the alloy and the parameter ϵ represents the interfacial width, which is small compared to the characteristic length of the laboratory scale. In addition, $u_0 : \Omega \to \mathscr{R}$ is a given initial function, Ω is a bounded domain in $\mathscr{R}^d$ $(d = 2,3)$, $\partial\Omega$ denotes its boundary, n is the outward normal, T is a given time, and $f(u) = F'(u)$ for a given energy potential $F(u)$. The homogeneous Neumann boundary condition implies that no mass loss occurs across the boundary walls. An important feature of the Allen-Cahn and Cahn-Hilliard equations is that they can be viewed as the gradient flow of the Liapunov energy function

$$E(u) = \int_\Omega \left(\frac{1}{2}|\nabla u|^2 + \frac{1}{\epsilon^2} F(u)\right) dx \tag{1.3}$$

in L^2-space and H^{-1}-space, respectively. By taking the inner product of Eq. (1.1) with $\Delta u + (1/\epsilon^2) f(u)$, the following energy law for Eq. (1.1) can be obtained:

$$\frac{\partial E(u(t))}{\partial t} = -\int_\Omega \left|-\Delta u + \frac{1}{\epsilon^2} f(u)\right|^2 dx. \tag{1.4}$$

Similarly, the energy law for Eq. (1.2) is given by

$$\frac{\partial E(u(t))}{\partial t} = -\int_\Omega \left|\nabla(-\Delta u + \frac{1}{\epsilon^2} f(u))\right|^2 dx. \tag{1.5}$$

Eqs. (1.4) and (1.5) indicate that the free energy decreases monotonically with time. The Allen-Cahn equation was originally introduced to describe the motion of anti-phase boundaries in crystalline solids [1], and the Cahn-Hilliard equation was introduced to describe the complicated phase separation and coarsening phenomena in a solid [7]. The two boundary conditions also imply that the mixture cannot pass through the boundary walls. The Allen-Cahn and Cahn-Hilliard equations have been employed in many complicated moving interface problems in materials science and fluid dynamics — e.g. see [3–5, 8, 11, 23]). As the numerical simulations have been very useful, it is very important to develop accurate and efficient numerical schemes for these phase field models. Note that an essential feature of Eqs. (1.1) and (1.2) is that they must satisfy the energy laws (1.4) and (1.5) respectively, so it is worthwhile to design efficient and accurate numerical schemes that satisfy similar energy decay properties.

It is known that explicit schemes usually lead to severe time step restrictions and also in general do not satisfy the energy decay property. A good alternative is to use implicit-explicit schemes that involve an elliptic equation with constant coefficients to be solved at each time step, making the implementation easy via fast elliptic solvers [2,6,17]. However, semi-implicit schemes usually have larger truncation errors and therefore require smaller time steps to guarantee accuracy as well as the energy stability. On the other hand, one can easily design an implicit scheme that satisfies energy stability and smaller truncation errors. The main disadvantage of the implicit approach is the need to solve nonlinear systems at each time step. Shen & Yang established the Lipschitz property for the special difference quotient of $f(u)$ and provided error estimates for two fully discretized implicit schemes with a spectral-Galerkin approximation in space [18]. Yang gave the stabilized semi-implicit scheme and the splitting scheme for the Allen-Cahn equation [22]. For the stabilized first-order scheme, Yang provided error analysis for the Allen-Cahn equation by using the spectrum estimate.

In Ref. [10], we presented a class of nonlinearly stable implicit-explicit methods for the Allen-Cahn equation. Our stabilized implicit-explicit schemes are shown to satisfy energy stability, which can relax the time step restrictions for the standard implicit-explicit methods. The present work can be regarded as an extension of Ref. [10], as the proposed methods discussed there will be extended to the Cahn-Hilliard equation (1.2). Moreover, rigorous error analysis will be established in this work.

There have been extensive efforts for investigating properties of numerical schemes for (1.1) and (1.2). Du and Nicolaides derived a second-order accurate unconditionally stable time-stepping nonlinear scheme for the Cahn-Hilliard equation by using the standard conforming finite element method [8]. Later on, Eyre derived a first-order accurate unconditionally stable time-stepping scheme for the Cahn-Hilliard equation [9], which has been used extensively by the computational community and has inspired many other time integration schemes. Other significant works that deal with the Cahn-Hilliard equation include Gomez & Hughes [11], He *et al.* [12], and Qiao *et al.* [24]. Other noteworthy contributions for the phase-field crystal equation and bistable epitaxial thin film equations include Xu & Tang [21], Li & Liu [14], Shen & Yang [19], Qiao *et al.* [15,16], and Wise *et al.* [13,20].

In this article, we restrict our attention to potential functions $F(u)$ with derivative $f(u) = F'(u)$ satisfying the condition that there exists a positive constant L such that

$$\max_{u\in\mathscr{R}} |f'(u)| \le L\ . \tag{1.6}$$

We study the stabilized Crank-Nicolson/Adams-Bashforth (CN/AB) scheme for the Allen-Cahn and Cahn-Hilliard equations. We use the standard conforming finite element method for the spatial discretization, and specify the range of the stabilization parameters involved to fulfil the nonlinear energy stability requirement. Optimal error estimates of the proposed second-order scheme are obtained, and the predicted theoretical results are then verified by a number of numerical experiments.

The rest of the paper is organized as follows. In Section 2, we consider the Allen-Cahn equation with a stabilized Crank-Nicolson/Adams-Bashforth (CN/AB) time discretization.

The optimal error estimate of the second-order CN/AB scheme is established for the Allen-Cahn equation. Similar analysis is provided in Section 3 for the Cahn-Hilliard equation (1.2). Section 4 is devoted to some numerical experiments, and some concluding remarks are made in the final section.

2. The Allen-Cahn Equation

We first introduce some notation and the standard Sobolev spaces. The space $L^2(\Omega)$ is equipped with the L^2-scalar product $(\cdot,\cdot)$ and L^2-norm $\|\cdot\|_0$. The space $H_0^1(\Omega)$ is endowed with the usual scalar product $(\nabla u,\nabla v)$ and the norm $\|\nabla u\|_0$. We also denote by $\|\cdot\|_r = \|\cdot\|_{0,r}$ the norm on space $L^r(\Omega)$ with $1<r<\infty$, and $\|\cdot\|_{k,r}$ the norm on space $W^{k,r}(\Omega)$ with $k=0,1,2,\cdots$. Given $q\in[1,\infty)$, $T>0$ and a Banach space W, the space $L^q(0,T;W)$ consists of functions defined on $(0,T)$ into W that are strongly q-integrable. The space $L^q(0,T;W)$ is equipped with the usual scalar product and norm

$$\|\cdot\|_{L^q(0,T;W)} = \left(\int_0^T \|\cdot\|_W^q\right)^{1/q}, \qquad (\cdot,\cdot) = \int_0^T (\cdot,\cdot)_W \, dt\,.$$

Based on the above definitions, the variational formulation for the Allen-Cahn equation (1.1) is to find $u\in L^2(0,T;H^1(\Omega))$ such that

$$\left(\frac{\partial u}{\partial t},v\right) + (\nabla u,\nabla v) + \frac{1}{\epsilon^2}(f(u),v) = 0\,, \quad \forall v\in L^2(0,T;H^1(\Omega))\,. \tag{2.1}$$

Let $t_n = n\delta t$ $(n=0,1,\cdots,N)$, where $\delta t = T/N$ denotes the time step size and N is an integer. u^n is an approximation to $u(x,t_n) =: u(t_n)$. In this work, we consider a second-order time discretization scheme for solving phase field models. In order to obtain high-order numerical schemes, Xu & Tang designed stabilized high-order time discretization schemes for the epitaxial growth model [21] . Their stability proof is based on the assumptions of the boundedness of numerical solution which cannot be verified a priori. Note that Shen & Yang used a similar stabilizing technique and also presented a stabilized second-order implicit-explicit scheme based on the classical second-order backward difference formula (BDF), by adding the second-order stabilized term $(S/\epsilon^2)(u^{n+1}-2u^n+u^{n-1})$ — viz. [18]

$$\begin{aligned}\frac{1}{2\delta t}(3u^{n+1}-4u^n+u^{n-1},v) + \frac{S}{\epsilon^2}(u^{n+1}-2u^n+u^{n-1},v) + (\nabla u^{n+1},\nabla v)\\ + \frac{1}{\epsilon^2}(2f(u^n)-f(u^{n-1}),v) = 0\,, \quad \forall v\in H^1(\Omega)\,.\end{aligned} \tag{2.2}$$

In scheme (2.2), under the condition

$$\delta t \le \frac{2\epsilon^2}{3L} \tag{2.3}$$

and $S \geq 0$, the following energy stability property holds:

$$E(u^{n+1}) + \left(\frac{1}{4\delta t} + \frac{S+L}{2\epsilon^2}\right)\|u^{n+1} - u^n\|_0^2$$
$$\leq E(u^n) + \left(\frac{1}{4\delta t} + \frac{S+L}{2\epsilon^2}\right)\|u^n - u^{n-1}\|_0^2\,, \quad \forall n \geq 1\,. \tag{2.4}$$

In order to relax the restriction on the time step (2.3), we consider the following two stabilized Crank-Nicolson/Adam-Bashforth (CN/AB) schemes.

Algorithm 2.1. (Stabilized second-order CN/AB scheme for AC equation)
Find $u^{n+1} \in H^1(\Omega)$, such that

$$\frac{1}{\delta t}\left(u^{n+1} - u^n, v\right) + \frac{1}{2}\left(\nabla(u^{n+1} + u^n), \nabla v\right) + \frac{S}{\epsilon^2}\left(u^{n+1} - 2u^n + u^{n-1}, v\right)$$
$$+\frac{1}{\epsilon^2}\left(\frac{3}{2}f(u^n) - \frac{1}{2}f(u^{n-1}), v\right) = 0\,, \quad \forall v \in H^1(\Omega)\,. \tag{2.5}$$

Note that the above scheme is (formally) second-order accurate in time.

Lemma 2.1. *If the condition* (1.6) *is satisfied and*

$$\delta t \leq \frac{\epsilon^2}{L} \tag{2.6}$$

where L is given by (1.6)*, then the following energy stability property for* Algorithm 2.1 *holds for any $S \geq 0$:*

$$\tilde{E}(u^{n+1}) \leq \tilde{E}(u^n)\,, \quad \forall n \geq 1\,, \tag{2.7}$$

where

$$\tilde{E}(u^n) := E(u^n) + \frac{L+2S}{4\epsilon^2}\|u^n - u^{n-1}\|_0^2\,.$$

Proof. On taking $v = u^{n+1} - u^n$ in (2.5) and using Taylor's theorem with remainder in the integral form, we obtain

$$F(u^{n+1}) - F(u^n) = (u^{n+1} - u^n)f(u^n) + \int_{u^n}^{u^{n+1}} (u^n - t)f'(t)dt\,,$$

which yields

$$E(u^{n+1}) - E(u^n) + \frac{1}{\delta t}\|u^{n+1} - u^n\|_0^2$$
$$+\frac{S}{2\epsilon^2}\left(\|u^{n+1} - u^n\|_0^2 - \|u^n - u^{n-1}\|_0^2 + \|u^{n+1} - 2u^n + u^{n-1}\|_0^2\right)$$
$$= \frac{1}{\epsilon^2}\left(\int_{u^n}^{u^{n+1}} f'(s)(u^{n+1} - s)ds\,, 1\right) - \frac{1}{2\epsilon^2}\left(\int_{u^{n-1}}^{u^n} f'(s)ds\,, u^{n+1} - u^n\right). \tag{2.8}$$

Then using condition (1.6) and the standard Cauchy-Schwarz inequality gives

$$\begin{aligned}\text{RHS of (2.8)} \leq & \frac{L}{2\epsilon^2}\left(\|u^{n+1}-u^n\|_0^2+\|u^{n+1}-u^n\|_0\|u^n-u^{n-1}\|_0\right)\\ \leq & \frac{L}{2\epsilon^2}\left(\frac{3}{2}\|u^{n+1}-u^n\|_0^2+\frac{1}{2}\|u^n-u^{n-1}\|_0^2\right), \end{aligned} \tag{2.9}$$

which together with the assumption (2.6), leads to the desired result (2.7). □

From (2.6), we see that the time step restriction of the stabilized second-order CN/AB schemes is one and half times larger than that given in (2.3). Moreover, we can also use the following stabilized CN/AB scheme.

Algorithm 2.2. Find $u^{n+1}\in H^1(\Omega)$, such that

$$\begin{aligned}&\frac{1}{\delta t}\left(u^{n+1}-u^n,v\right)+\frac{1}{2}\left(\nabla(u^{n+1}+u^n),\nabla v\right)+\frac{S\delta t}{\epsilon^2}\left(u^{n+1}-u^n,v\right)\\ &\quad+\frac{1}{\epsilon^2}\left(\frac{3}{2}f(u^n)-\frac{1}{2}f(u^{n-1}),v\right)=0\,,\quad \forall v\in H^1(\Omega)\,. \end{aligned} \tag{2.10}$$

Note that the above scheme is also of second-order accuracy in time.

Lemma 2.2. *If the condition* (1.6) *is satisfied and*

$$S\geq\frac{L^2}{4\epsilon^2}\,, \tag{2.11}$$

where L is given by (1.6)*, then the following energy stability property for* Algorithm 2.2 *holds:*

$$\tilde{E}(u^{n+1})\leq\tilde{E}(u^n)\,,\quad \forall n\geq 1\,, \tag{2.12}$$

for any time step size δt, where

$$\tilde{E}(u^n):=E(u^n)+\frac{L}{4\epsilon^2}\|u^n-u^{n-1}\|_0^2\,.$$

Proof. Similar to the analysis for Lemma 2.1, the following result holds:

$$\begin{aligned}&E(u^{n+1})-E(u^n)+\left(\frac{1}{\delta t}+\frac{4S\delta t-3L}{4\epsilon^2}\right)\|u^{n+1}-u^n\|_0^2\\ &\leq\frac{L}{4\epsilon^2}\|u^n-u^{n-1}\|_0^2\,,\quad \forall n\geq 1\,. \end{aligned} \tag{2.13}$$

To ensure energy stability, we require the conditions

$$\frac{1}{\delta t}+\frac{4S\delta t-3L}{4\epsilon^2}\geq 0\quad\text{and}\quad\frac{1}{\delta t}+\frac{S\delta t-L}{\epsilon^2}\geq 0\,,$$

or equivalently

$$\left(\delta t-\frac{3L}{8S}\right)^2+\frac{\epsilon^2}{S}-\frac{9L^2}{64S^2}\geq 0\quad\text{and}\quad\left(\delta t-\frac{L}{2S}\right)^2+\frac{\epsilon^2}{S}-\frac{L^2}{4S^2}\geq 0\,,$$

which is satisfied provided that condition (2.11) holds. □

Next, we consider a fully discretized version of Algorithm 2.1 by using the finite element approximation for the spatial variables. Let $h > 0$ be a real positive parameter. The finite element subspace U_h of $H^1(\Omega)$ is characterized by $J_h = J_h(\Omega)$, a partitioning of $\overline{\Omega}$ into triangles or quadrilaterals, assumed to be uniformly regular as $h \to 0$. Let $P_h : L^2(\Omega) \to U_h$ denote the L^2-orthogonal projection such that

$$(P_h v, v_h) = (v, v_h)\,, \qquad v \in L^2(\Omega), \quad v_h \in U_h\,,$$

and let us define a projection operator $I_h : H^1(\Omega) \to U_h$ by

$$(\nabla(v - I_h v), \nabla\varphi) = 0\,, \qquad (v - I_h v, 1) = 0\,, \quad \forall \varphi \in U_h\,.$$

It is well known that the following estimates hold:

$$\begin{aligned} &\|v - P_h v\|_0 \le c h^m \|v\|_m, && \forall v \in H^m(\Omega),\ m \ge 0,\\ &\|v - I_h v\|_i \le c h^{m-i} \|v\|_m,\ i = 0, 1; && \forall v \in H^m(\Omega),\ m \ge 1. \end{aligned}$$

We define $u_h^0 = P_h u_0$ and find $u_h^{n+1} \in U_h$, $1 \le n \le N-1$ by the following fully discretized scheme:

$$\begin{aligned} &\frac{1}{\delta t}\left(u_h^{n+1} - u_h^n, v_h\right) + \frac{1}{2}\left(\nabla(u_h^{n+1} + u_h^n), \nabla v_h\right) + \frac{S}{\epsilon^2}\left(u_h^{n+1} - 2u_h^n + u_h^{n-1}, v_h\right)\\ &\quad + \frac{1}{\epsilon^2}\left(\frac{3}{2} f(u_h^n) - \frac{1}{2} f(u_h^{n-1}), v_h\right) = 0\,, \quad \forall v_h \in U_h\,, \end{aligned} \tag{2.14}$$

where u_h^n denotes the finite element approximation of u^n. Now we establish error estimates for the fully discrete schemes. In our proof, C (with or without a subscript) will denote a positive constant, which may take different values at different places.

Theorem 2.1. *Consider the fully discretized version of* Algorithm 2.1*,* (2.14)*, which uses the standard conforming finite element approximation for the spatial variables. Let us assume that* $u \in \mathscr{C}(0, T; H^m(\Omega))$*,* $u_t \in L^2(0, T; H^m(\Omega)) \bigcap L^2(0, T; L^2(\Omega))$*,* $u_{tt} \in L^2(0, T; H^1(\Omega))$ *and* $u_{ttt} \in L^2(0, T; H^{-1}(\Omega))$*. Under the conditions* (1.6) *and* (2.6)*, the following error estimate holds:*

$$\begin{aligned} &\|u(t_n) - u_h^n\|_0 \le C(\delta t^2 + h^2)\,,\\ &\left(\delta t \sum_{k=0}^{n} \left\| \nabla(u(t_{k+\frac{1}{2}}) - \frac{1}{2}(u_h^{k+1} + u_h^k)) \right\|_0^2 \right)^{\frac{1}{2}} \le C(\delta t^2 + h)\,, \end{aligned} \tag{2.15}$$

where C is a positive constant that depends on ε, T, and u and its derivatives.

Proof. We write $u(t_n) = u(\cdot, t_n)$ and denote

$$\begin{aligned} &\widehat{e}^n = u(t_n) - I_h u(t_n)\,, && e^n = I_h u(t_n) - u_h^n\,,\\ &\overline{e}^n = u(t_n) - u_h^n = \widehat{e}^n + e^n\,, && e^{n+\frac{1}{2}} = \frac{1}{2}(e^n + e^{n+1})\,. \end{aligned}$$

Define the truncation error

$$R_1^{n+\frac{1}{2}} := \frac{u(t_{n+1})-u(t_n)}{\delta t} - u_t(t_{n+\frac{1}{2}}),$$
$$R_2^{n+\frac{1}{2}} := \Delta u(t_{n+\frac{1}{2}}) - \Delta\left(\frac{u(t_{n+1})+u(t_n)}{2}\right).$$

By using the Taylor expansion with integral residual, it is easy to show that

$$\|R_1^{n+\frac{1}{2}}\|_s^2 \le \delta t^3 \int_{t_n}^{t_{n+1}} \|u_{ttt}(t)\|_s^2 dt, \quad s=-1,0, \tag{2.16}$$
$$\|R_2^{n+\frac{1}{2}}\|_s^2 \le \delta t^3 \int_{t_n}^{t_{n+1}} \|u_{tt}(t)\|_{s+2}^2 dt, \quad s=-1,0. \tag{2.17}$$

Subtracting Eq. (2.14) from Eq. (2.1) at $t^{n+1/2}$ gives

$$\begin{aligned}
&\frac{1}{\delta t}\left(e^{n+1}-e^n, v_h\right) + \left(\nabla e^{n+\frac{1}{2}}, \nabla v_h\right) + \frac{S}{\epsilon^2}\left(e^{n+1}-2e^n+e^{n-1}, v_h\right)\\
&= \left(R_1^{n+\frac{1}{2}} + R_2^{n+\frac{1}{2}}, v_h\right) + \frac{1}{\delta t}(I-I_h)\left(u(t_{n+1})-u(t_n), v_h\right)\\
&\quad + \frac{S}{\epsilon^2}\left(u(t_{n+1})-2u(t_n)+u(t_{n-1}), v_h\right) - \frac{S}{\epsilon^2}(I-I_h)\left(u(t_{n+1})-2u(t_n)+u(t_{n-1}), v_h\right)\\
&\quad + \frac{1}{\epsilon^2}\left(f(u(t_{n+\frac{1}{2}})) - \frac{3}{2}f(u_h^n) + \frac{1}{2}f(u_h^{n-1}), v_h\right).
\end{aligned} \tag{2.18}$$

Taking $v_h = 2\delta t e^{n+\frac{1}{2}}$ in Eq. (2.18) yields

$$\begin{aligned}
&\left(1+\frac{S\delta t}{2\epsilon^2}\right)\left(\|e^{n+1}\|_0^2 - \|e^n\|_0^2\right) + 2\delta t\|\nabla e^{n+\frac{1}{2}}\|_0^2\\
&= 2\delta t\left(R_1^{n+\frac{1}{2}} + R_2^{n+\frac{1}{2}}, e^{n+\frac{1}{2}}\right) + 2\left((I-I_h)(u(t_{n+1})-u(t_n)), e^{n+\frac{1}{2}}\right)\\
&\quad + \frac{2\delta tS}{\epsilon^2}\left(u(t_{n+1})-2u(t_n)+u(t_{n-1}), e^{n+\frac{1}{2}}\right)\\
&\quad - \frac{2\delta tS}{\epsilon^2}\left((I-I_h)(u(t_{n+1})-2u(t_n)+u(t_{n-1})), e^{n+\frac{1}{2}}\right)\\
&\quad + \frac{2\delta tS}{\epsilon^2}\left(e^n-e^{n-1}, e^{n+\frac{1}{2}}\right) + \frac{2\delta t}{\epsilon^2}\left(f(u(t_{n+\frac{1}{2}})) - \frac{3}{2}f(u_h^n) + \frac{1}{2}f(u_h^{n-1}), e^{n+\frac{1}{2}}\right)\\
&=: \sum_{i=1}^{6} I_i.
\end{aligned} \tag{2.19}$$

We next estimate the terms I_i $(i=1,\cdots,6)$ on the right-hand side, respectively. For I_1,

on using the Young inequality and the Cauchy-Schwarz inequality we obtain

$$\begin{aligned} I_1 &\le 2\delta t \|R_1^{n+\frac{1}{2}} + R_2^{n+\frac{1}{2}}\|_{-1} \|e^{n+\frac{1}{2}}\|_1 \\ &\le \delta t \|\nabla e^{n+\frac{1}{2}}\|_0^2 + C\delta t \left(\|R_1^{n+\frac{1}{2}}\|_{-1}^2 + \|R_2^{n+\frac{1}{2}}\|_{-1}^2 \right) . \end{aligned} \tag{2.20}$$

For I_2, using the Young inequality and the integral identity, we have

$$\begin{aligned} I_2 &\le 2\|(I - I_h)(u(t_{n+1}) - u(t_n))\|_0 \|e^{n+\frac{1}{2}}\|_0 \\ &\le \frac{\delta t}{\epsilon^2} \|e^{n+\frac{1}{2}}\|_0^2 + C\epsilon^2 \int_{t_n}^{t_{n+1}} \|(I - I_h)u_t(s)\|_0^2 ds . \end{aligned} \tag{2.21}$$

For I_3 and I_4, using the Young inequality and the Taylor expansion with integral residual we have

$$\begin{aligned} I_3 &\le \frac{2\delta t S}{\epsilon^2} \|u(t_{n+1}) - 2u(t_n) + u(t_{n-1})\|_0 \|e^{n+\frac{1}{2}}\|_0 \\ &\le \frac{\delta t}{\epsilon^2} \|e^{n+\frac{1}{2}}\|_0^2 + \frac{CS^2 \delta t^4}{\epsilon^2} \int_{t_{n-1}}^{t_{n+1}} \|u_{tt}(s)\|_0^2 ds \text{ ; and} \end{aligned} \tag{2.22}$$

$$\begin{aligned} I_4 &\le \frac{2\delta t S}{\epsilon^2} \|(I - I_h)(u(t_{n+1}) - 2u(t_n) + u(t_{n-1}))\|_0 \|e^{n+\frac{1}{2}}\|_0 \\ &\le \frac{\delta t}{\epsilon^2} \|e^{n+\frac{1}{2}}\|_0^2 + \frac{CS^2 \delta t^4}{\epsilon^2} \int_{t_{n-1}}^{t_{n+1}} \|(I - I_h)u_{tt}(s)\|_0^2 ds . \end{aligned} \tag{2.23}$$

Moreover, using the Young inequality for I_5 gives

$$\begin{aligned} I_5 &\le \frac{2\delta t S}{\epsilon^2} \|e^n - e^{n-1}\|_0 \|e^{n+\frac{1}{2}}\|_0 \\ &\le \frac{\delta t}{\epsilon^2} \|e^{n+\frac{1}{2}}\|_0^2 + \frac{CS^2 \delta t}{\epsilon^2} \|e^n - e^{n-1}\|_0^2 . \end{aligned} \tag{2.24}$$

The last term is more complicated:

$$\begin{aligned} I_6 &\le \frac{2\delta t}{\epsilon^2} \left\| f(u(t_{n+\frac{1}{2}})) - \frac{3}{2} f(u_h^n) + \frac{1}{2} f(u_h^{n-1}) \right\|_0 \|e^{n+\frac{1}{2}}\|_0 \\ &\le \frac{\delta t}{\epsilon^2} \|e^{n+\frac{1}{2}}\|_0^2 + \frac{\delta t}{\epsilon^2} \left\| f(u(t_{n+\frac{1}{2}})) - \frac{3}{2} f(u_h^n) + \frac{1}{2} f(u_h^{n-1}) \right\|_0^2 \\ &=: \frac{\delta t}{\epsilon^2} \|e^{n+\frac{1}{2}}\|_0^2 + \frac{\delta t}{\epsilon^2} I_7 , \end{aligned} \tag{2.25}$$

where

$$
\begin{aligned}
I_7 \le & \left\| f(u(t_{n+\frac{1}{2}})) - \frac{3}{2} f(u(t_n)) + \frac{1}{2} f(u(t_{n-1})) \right\|_0^2 \\
& + \left\| \frac{3}{2} f(u(t_n)) - \frac{3}{2} f(u_h^n) - \frac{1}{2} f(u(t_{n-1})) + \frac{1}{2} f(u_h^{n-1}) \right\|_0^2 \\
\le & \left\| f(u(t_{n+\frac{1}{2}})) - \frac{1}{2} (f(u(t_{n+1})) + f(u(t_n))) \right\|_0^2 \\
& + \left\| \frac{1}{2} (f(u(t_{n+1})) + f(u(t_n))) - \frac{3}{2} f(u(t_n)) + \frac{1}{2} f(u(t_{n-1})) \right\|_0^2 \\
& + CL^2 (\|u(t_n) - u_h^n\|_0^2 + \|u(t_{n-1}) - u_h^{n-1}\|_0^2) \\
\le & CL\delta t^3 \int_{t_{n-1}}^{t_{n+1}} \|u_{tt}(s)\|_0^2 ds + CL^2 \left(\|e^n\|_0^2 + \|\widehat{e}^n\|_0^2 + \|e^{n-1}\|_0^2 + \|\widehat{e}^{n-1}\|_0^2 \right), \qquad (2.26)
\end{aligned}
$$

in which we have used the Taylor expansion with integral residual, the Cauchy-Schwarz inequality and the relationship $\|u(t_n) - u_h^n\|_0^2 = \|\widehat{e}^n + e^n\|_0^2 \le 2(\|\widehat{e}^n\|_0^2 + \|e^n\|_0^2)$. Combining these into Eq. (2.19) and using inequalities (2.16) yields

$$
\begin{aligned}
& \left(1 + \frac{S\delta t}{2\epsilon^2} \right) (\|e^{n+1}\|_0^2 - \|e^n\|_0^2) + \delta t \|\nabla e^{n+\frac{1}{2}}\|_0^2 \\
& \le C\delta t \left(\|R_1^{n+\frac{1}{2}}\|_{-1}^2 + \|R_2^{n+\frac{1}{2}}\|_{-1}^2 \right) + C\epsilon^2 \int_{t_n}^{t_{n+1}} \|(I - I_h) u_t(s)\|_0^2 ds \\
& \quad + \frac{C\delta t^4}{\epsilon^2} \int_{t_{n-1}}^{t_{n+1}} \|u_{tt}(s)\|_0^2 ds + \frac{CS^2 \delta t^4}{\epsilon^2} \int_{t_{n-1}}^{t_{n+1}} \|(I - I_h) u_{tt}(s)\|_0^2 ds \\
& \quad + \frac{C\delta t}{\epsilon^2} \left(\|e^n\|_0^2 + \|\widehat{e}^n\|_0^2 + \|e^{n-1}\|_0^2 + \|\widehat{e}^{n-1}\|_0^2 \right). \qquad (2.27)
\end{aligned}
$$

On summing up the above inequality for $1 \le n \le N-1$ and using the interpolation error estimate, we therefore obtain

$$
\begin{aligned}
& \left(1 + \frac{S\delta t}{2\epsilon^2} \right) \left(\|e^N\|_0^2 - \|e^1\|_0^2 \right) + \delta t \sum_{n=1}^{N-1} \|\nabla e^{n+\frac{1}{2}}\|_0^2 \\
& \le C\delta t^4 \left(\|u_{ttt}\|_{L^2(0,T;H^{-1})} + \|u_{tt}\|_{L^2(0,T;H^1)} + C\epsilon^2 h^2 \|u_t\|_{L^2(0,T;H^1)}^2 \right) \\
& \quad + \frac{C\delta t^4}{\epsilon^2} \left(\|u_{tt}\|_{L^2(0,T;L^2)}^2 + h^2 \|u_{tt}\|_{L^2(0,T;L^2)}^2 \right) \\
& \quad + \frac{C\delta t}{\epsilon^2} \sum_{n=0}^{N-1} \left(\|e^n\|_0^2 + \|\widehat{e}^n\|_0^2 + \|e^{n-1}\|_0^2 + \|\widehat{e}^{n-1}\|_0^2 \right). \qquad (2.28)
\end{aligned}
$$

The result (2.15) then follows by using the discrete Gronwall inequality and the triangular inequality $\|\overline{e}^n\|_i \le \|\widehat{e}^n\|_i + \|e^n\|_i$ $(i = 0, 1)$. □

Similar results for Algorithm 2.2 can be obtained by using the same techniques as above, so the relevant details are omitted here.

3. The Cahn-Hilliard Equations

The mixed variational formulation for the Cahn-Hilliard equations is to find u, $w \in L^2(0,T;H^1(\Omega))$ such that

$$\begin{cases} \left(\dfrac{\partial u}{\partial t}, v\right) + (\nabla w, \nabla v) = 0\,, & \forall v \in L^2(0,T;H^1(\Omega))\,, \\ (\nabla u, \nabla \phi) + \dfrac{1}{\epsilon^2}(f(u),\phi) = (w,\phi)\,, & \forall \phi \in L^2(0,T;H^1(\Omega))\,. \end{cases} \tag{3.1}$$

Shen & Yang [18] obtained a stabilized second-order implicit-explicit scheme from the classical second-order BDF scheme, by adding the term $(S/\epsilon^2)(u^{n+1}-2u^n+u^{n-1})$ in the second equation of (3.1). Their stability analysis requires some very detailed energy estimates, and below we propose two stabilized second-order CN/AB schemes where the theoretical analysis is relatively simple.

Algorithm 3.1. (Stabilized second-order CN/AB scheme for CH equation)
Find $(u^{n+1}, w^{n+1}) \in H^1(\Omega)\times H^1(\Omega)$, such that

$$\begin{cases} \dfrac{1}{\delta t}(u^{n+1}-u^n, v) + (\nabla w^{n+1}, \nabla v) = 0\,, \\ \dfrac{1}{2}\left(\nabla(u^{n+1}+u^n), \nabla\phi\right) + \dfrac{S\delta t}{\epsilon^2}(u^{n+1}-u^n,\phi) \\ \qquad\qquad + \dfrac{1}{\epsilon^2}\left(\dfrac{3}{2}f(u^n) - \dfrac{1}{2}f(u^{n-1}), \phi\right) = (w^{n+1},\phi)\,, \end{cases} \tag{3.2}$$

for all $(v,\phi)\in H^1(\Omega)\times H^1(\Omega)$.
Note the above algorithm gives a second-order time discretization scheme.

Lemma 3.1. *Under the condition*

$$\delta t \geq \frac{L}{S}\,, \tag{3.3}$$

the following energy stability property for Algorithm 3.1 *holds:*

$$E(u^{n+1}) + \delta t\|\nabla w^{n+1}\|_0^2 + \frac{L}{4\epsilon^2}\|u^{n+1}-u^n\|_0^2 \leq E(u^n) + \frac{L}{4\epsilon^2}\|u^n-u^{n-1}\|_0^2\,. \tag{3.4}$$

Proof. On taking $v = w^{n+1}$ and $\phi = u^{n+1}-u^n$ in (3.2) and using the Taylor expansion with integral residual, we have

$$(u^{n+1}-u^n, w^{n+1}) + \delta t\|\nabla w^{n+1}\|_0^2 = 0\,,$$

and

$$E(u^{n+1})-E(u^n)+\frac{S\delta t}{\epsilon^2}\|u^{n+1}-u^n\|_0^2 \\ -\frac{1}{\epsilon^2}\left(\int_{u^n}^{u^{n+1}} f'(t)(u^{n+1}-t)dt,1\right)+\frac{1}{2\epsilon^2}\left(\int_{u^{n-1}}^{u^n} f'(t)dt,u^{n+1}-u^n\right) \\ =\left(w^{n+1},u^{n+1}-u^n\right). \tag{3.5}$$

Consequently,

$$E(u^{n+1})-E(u^n)+\frac{S\delta t}{\epsilon^2}\|u^{n+1}-u^n\|_0^2+\delta t\|\nabla w^{n+1}\|_0^2 \\ \le\frac{L}{2\epsilon^2}\left(\frac{3}{2}\|u^{n+1}-u^n\|_0^2+\frac{1}{2}\|u^n-u^{n-1}\|_0^2\right), \tag{3.6}$$

which implies the desired result (3.4). □

Algorithm 3.2. Find $(u^{n+1},w^{n+1})\in H^1(\Omega)\times H^1(\Omega)$, such that

$$\begin{cases} \dfrac{1}{\delta t}(u^{n+1}-u^n,v)+(\nabla w^{n+1},\nabla v)=0\,, \\ \dfrac{1}{2}\left(\nabla(u^{n+1}+u^n),\nabla\phi\right)+\dfrac{S}{\epsilon^2}(u^{n+1}-2u^n+u^{n-1},\phi) \\ \qquad\qquad +\dfrac{1}{\epsilon^2}\left(\dfrac{3}{2}f(u^n)-\dfrac{1}{2}f(u^{n-1}),\phi\right)=(w^{n+1},\phi)\,, \end{cases} \tag{3.7}$$

for all $(v,\phi)\in H^1(\Omega)\times H^1(\Omega)$.
Note the above algorithm is also second-order accurate in time.

We next use a finite element approximation for the spatial variables, and establish error estimates for the fully discrete versions of Algorithm 3.1: Given $u_h^0=P_hu_0$, find $(u_h^{n+1},w_h^{n+1})\in U_h\times U_h$ such that for all $(v_h,\phi_h)\in U_h\times U_h$,

$$\begin{cases} \dfrac{1}{\delta t}(u_h^{n+1}-u_h^n,v_h)+(\nabla w_h^{n+1},\nabla v_h)=0\,, \\ \dfrac{1}{2}\left(\nabla(u_h^{n+1}+u_h^n),\nabla\phi_h\right)+\dfrac{S\delta t}{\epsilon^2}(u_h^{n+1}-u_h^n,\phi_h) \\ \qquad\qquad +\dfrac{1}{\epsilon^2}\left(\dfrac{3}{2}f(u_h^n)-\dfrac{1}{2}f(u_h^{n-1}),\phi_h\right)=(w_h^{n+1},\phi_h\right). \end{cases} \tag{3.8}$$

We denote

$$\begin{aligned} &\bar e^n=u(t_n)-I_hu(t_n)\,, && e^n=I_hu(t_n)-u_h^n\,, \\ &\bar\eta^n=w(t_n)-I_hw(t_n)\,, && \eta^n=I_hw(t_n)-w_h^n\,, \\ &\bar\eta^{n+\frac12}=I_hw(t_{n+\frac12})-w_h^{n+1}\,, && \eta^{n+\frac12}=w(t_{n+\frac12})-I_hw(t_{n+\frac12})\,. \end{aligned}$$

Theorem 3.1. *Consider the fully discretized scheme* (3.8)*, which uses the standard conforming finite element approximation for the spatial variables. Assuming that* $u, w \in \mathscr{C}(0,T;H^1(\Omega))$*,* $u_t \in L^2(0,T;H^1(\Omega)) \bigcap L^2(0,T;L^2(\Omega))$*,* $u_{tt} \in L^2(0,T;H^1(\Omega))$ *and* $u_{ttt} \in L^2(0,T;H^{-1}(\Omega))$*. under the conditions* (1.6) *and* (3.3) *the following error estimate holds:*

$$\|u(t_n) - u_h^n\|_0 + \left(\delta t \sum_{k=0}^{n} \|w(t_{k+\frac{1}{2}}) - \frac{1}{2}(w_h^{k+1} + w_h^k)\|_0^2 \right)^{\frac{1}{2}} \le C(\delta t^2 + h^2)\,, \tag{3.9}$$

where C *is a positive constant that depends on* ε*,* T*, and* u *and its derivatives.*

Proof. Subtracting (3.1) from (3.8) at $t^{n+\frac{1}{2}}$ gives

$$\begin{aligned} &\left(\frac{e^{n+1}-e^n}{\delta t}, v_h\right) + \left(\nabla \eta^{n+\frac{1}{2}}, \nabla v_h\right) \\ &\quad = \left(R_1^{n+\frac{1}{2}}, v_h\right) - \left(\nabla \bar{\eta}^{n+\frac{1}{2}}, \nabla v_h\right) - \left(\frac{\bar{e}^{n+1}-\bar{e}^n}{\delta t}, v_h\right), \end{aligned} \tag{3.10}$$

and

$$\begin{aligned} &\left(\nabla e^{n+\frac{1}{2}}, \nabla \phi_h\right) + \frac{1}{\epsilon^2}\left(f(u(t_{n+\frac{1}{2}})) - \frac{3}{2}f(u_h^n) + \frac{1}{2}f(u_h^{n-1}), \phi_h\right) + \frac{S\delta t}{\epsilon^2}\left(e^{n+1}-e^n, \phi_h\right) \\ &= \left(R_2^{n+\frac{1}{2}}, \phi_h\right) + \left(\eta^{n+\frac{1}{2}} + \bar{\eta}^{n+\frac{1}{2}}, \phi_h\right) - \left(\nabla \bar{e}^{n+\frac{1}{2}}, \nabla \phi_h\right) + \frac{S\delta t}{\epsilon^2}\left(u(t_{n+1}) - u(t_n), \phi_h\right) \\ &\quad - \frac{S\delta}{\epsilon^2}\left((I - I_h)(u(t_{n+1}) - u(t_n)), \phi_h\right). \end{aligned} \tag{3.11}$$

On taking $v_h = 2\delta t e^{n+1/2}$ in Eq. (3.10) and $\phi_h = -2\delta t \eta^{n+1/2}$ in Eq. (3.11), and then summing up the resulting identities, we have

$$\begin{aligned} &\|e^{n+1}\|_0^2 - \|e^n\|_0^2 + 2\delta t \|\eta^{n+\frac{1}{2}}\|_0^2 \\ &= 2\delta t \left(R_1^{n+\frac{1}{2}}, e^{n+\frac{1}{2}}\right) - 2\left(\bar{e}^{n+1} - \bar{e}^n, e^{n+\frac{1}{2}}\right) + 2\delta t^2 \frac{S}{\epsilon^2}\left(e^{n+1} - e^n, \eta^{n+\frac{1}{2}}\right) \\ &\quad + 2\delta t \frac{1}{\epsilon^2}\left(f(u(t_{n+\frac{1}{2}})) - \frac{3}{2}f(u_h^n) + \frac{1}{2}f(u_h^{n-1}), \eta^{n+\frac{1}{2}}\right) - 2\delta t \left(R_2^{n+\frac{1}{2}}, \eta^{n+\frac{1}{2}}\right) \\ &\quad - 2\delta t \left(\bar{\eta}^{n+\frac{1}{2}}, \eta^{n+\frac{1}{2}}\right) - 2\delta t^2 \frac{S}{\epsilon^2}\left(u(t_{n+1}) - u(t_n), \eta^{n+\frac{1}{2}}\right) \\ &\quad + \delta t^2 \frac{S}{\epsilon^2}\left((I - I_h)(u(t_{n+1}) - u(t_n)), \eta^{n+\frac{1}{2}}\right) \\ &=: \sum_{i=1}^{8} \Pi_i\,. \end{aligned} \tag{3.12}$$

Next we estimate the right terms Π_i $(i = 1, \cdots, 8)$, respectively. The first term Π_1 can be estimated by using (2.16) with $s = -1$ and the Young inequality:

$$\Pi_1 \le C\delta t \|e^{n+\frac{1}{2}}\|_0^2 + C\delta t^4 \int_{t_n}^{t_{n+1}} \|u_{ttt}(s)\|_0^2 ds \,. \tag{3.13}$$

For the terms Π_2 and Π_3, on using the integral identity and the Young inequality respectively we obtain

$$\begin{aligned}
\Pi_2 &\le C\|e^{n+\frac{1}{2}}\|_0 \|(I - I_h)(u(t_{n+1}) - u(t_n))\|_0 \\
&\le C\delta t \|e^{n+\frac{1}{2}}\|_0^2 + C \int_{t_n}^{t_{n+1}} \|(I - I_h)u_t(s)\|_0^2 ds \,; \text{ and} \qquad (3.14) \\
\Pi_3 &\le 2\delta t^2 \frac{S}{\epsilon^2} \|e^{n+1} - e^n\|_0 \|\eta^{n+\frac{1}{2}}\|_0 \\
&\le \frac{\delta t^2}{8} \|\eta^{n+\frac{1}{2}}\|_0^2 + \frac{C\delta t^2 S^2}{\epsilon^4} \|e^{n+1} - e^n\|_0^2 \,. \qquad (3.15)
\end{aligned}$$

The estimate of Π_4 requires the Taylor expansion of $f(u)$ and regularity of $f(u)$ and u:

$$\begin{aligned}
\Pi_4 &\le 2\delta t \frac{1}{\epsilon^2} \|f(u(t_{n+\frac{1}{2}})) - \frac{3}{2} f(u_h^n) + \frac{1}{2} f(u_h^{n-1})\|_0 \|\eta^{n+\frac{1}{2}}\|_0 \\
&\le \frac{\delta t}{8} \|\eta^{n+\frac{1}{2}}\|_0^2 + \frac{C\delta t}{\epsilon^4} \|f(u(t_{n+\frac{1}{2}})) - \frac{3}{2} f(u_h^n) + \frac{1}{2} f(u_h^{n-1})\|_0^2 \\
&\le \frac{\delta t}{8} \|\eta^{n+\frac{1}{2}}\|_0^2 + \frac{C\delta t^4}{\epsilon^4} \int_{t_{n-1}}^{t_{n+1}} \|u_{tt}(s)\|_0^2 ds \\
&\quad + CL^2 \Big(\|e^n\|_0^2 + \|\widehat{e}^n\|_0^2 + \|e^{n-1}\|_0^2 + \|\widehat{e}^{n-1}\|_0^2 \Big) \,. \qquad (3.16)
\end{aligned}$$

For Π_5 and Π_6, on using (2.17) and the Young inequality respectively we get

$$\begin{aligned}
\Pi_5 &\le \frac{\delta t}{8} \|\eta^{n+\frac{1}{2}}\|_0^2 + C\delta t^4 \int_{t_n}^{t_{n+1}} \|u_{tt}(s)\|_0^2 ds \,, \text{ and} \qquad (3.17) \\
\Pi_6 &\le \frac{\delta t}{8} \|\eta^{n+\frac{1}{2}}\|_0^2 + C\delta t \|\bar{\eta}^{n+\frac{1}{2}}\|_0^2 \,. \qquad (3.18)
\end{aligned}$$

Further estimates on the remaining terms are

$$\begin{aligned}
\Pi_7 &\le 2\delta t^2 \frac{S}{\epsilon^2} \|u(t_{n+1}) - u(t_n)\|_0 \|\eta^{n+\frac{1}{2}}\|_0 \\
&\le \frac{\delta t}{8} \|\eta^{n+\frac{1}{2}}\|_0^2 + \frac{C\delta t^3 S}{\epsilon^4} \|u(t_{n+1}) - u(t_n)\|_0^2 \\
&\le \frac{\delta t}{8} \|\eta^{n+\frac{1}{2}}\|_0^2 + \frac{C\delta t^4 S}{\epsilon^4} \int_{t_n}^{t_{n+1}} \|u_t(s)\|_0^2 ds \,; \qquad (3.19)
\end{aligned}$$

and

$$\begin{aligned}\Pi_8 &\le \delta t^2 \frac{S}{\epsilon^2}\|(I-I_h)(u(t_{n+1})-u(t_n))\|_0\|\eta^{n+\frac{1}{2}}\|_0\\ &\le \frac{\delta t}{8}\|\eta^{n+\frac{1}{2}}\|_0^2+\frac{C\delta t^3 S}{\epsilon^4}\|(I-I_h)(u(t_{n+1})-u(t_n))\|_0^2\\ &\le \frac{\delta t}{8}\|\eta^{n+\frac{1}{2}}\|_0^2+\frac{C\delta t^4 S}{\epsilon^4}\int_{t_n}^{t_{n+1}}\|(I-I_h)u_t(s)\|_0^2 ds\,, \end{aligned} \tag{3.20}$$

where we have used the Young inequality and the integral identity. Putting the above estimates into Eq. (3.12) and using (2.16) yields

$$\begin{aligned}&\|e^{n+1}\|_0^2-\|e^n\|_0^2+\delta t\|\eta^{n+\frac{1}{2}}\|_0^2\\ &\le C\delta t\|e^{n+\frac{1}{2}}\|_0^2+C\delta t^4\int_{t_n}^{t_{n+1}}\|u_{ttt}(s)\|_0^2 ds+C\int_{t_n}^{t_{n+1}}\|(I-I_h)u_t(s)\|_0^2 ds\\ &\quad+\frac{C\delta t^2 S^2}{\epsilon^4}\|e^{n+1}-e^n\|_0^2+\frac{C\delta t^4 S}{\epsilon^4}\int_{t_n}^{t_{n+1}}\|u_t(s)\|_0^2 ds\\ &\quad+\frac{C\delta t^4 S}{\epsilon^4}\int_{t_n}^{t_{n+1}}\|(I-I_h)u_t(s)\|_0^2 ds\\ &\quad+CL^2\left(\|e^n\|_0^2+\|\widehat{e}^n\|_0^2+\|e^{n-1}\|_0^2+\|\widehat{e}^{n-1}\|_0^2\right)\,, \end{aligned} \tag{3.21}$$

which leads to the desired estimate (3.9). □

Similar results for Algorithm 3.2 may be estimated by using the same technique, so details are again omitted here.

4. Numerical Experiments

In this section, we present some numerical results to verify the previous theoretical results.

4.1. 2D Allen-Cahn equation

For the 2D Allen-Cahn equation, the initial condition is taken to be the very small amplitude trigonometric function

$$u_0(x,y)=0.05\sin x\sin y\,.$$

We consider a periodic boundary condition, and adopt the parameter $\epsilon=0.1$ and the solution domain $\Omega=[0,2\pi]\times[0,2\pi]$. This example is designed to study the accuracy and the efficiency of the CN/AB scheme.

We first test the numerical accuracy in time and space. Since the exact solution is unknown, we take as the “exact" solution the numerical result obtained on a P_1-conforming

element with the spatial step size $h = 2\pi/128$ and time step size $\delta t = 10^{-3}$. For $S = 0$ and $S = 1$ respectively, Table 1shows the L^2-errors at $T = 0.01$ obtained using different time steps. The numerical scheme evidently gives the optimal rate of convergence (viz. order 2) in the L^2-norm for this two-dimensional Allen-Cahn problem. By fixing the time step size be $\delta t = 10^{-4}$ (which is sufficiently small), we test the convergence for the spatial discretization. Table 2 shows the L^2-errors obtained using different spatial step sizes, and the expected rate of convergence is again observed. In both cases, it is found that the stabilization terms involving S do not affect the rate of convergence provided the mesh size is sufficiently small.

Table 1: Numerical results for the time discretization for the 2D Allen-Cahn equation with (a) $S = 0$ and (b) $S = 1$.

Time step	$\delta t = 10^{-3}$	$\delta t/2$	$\delta t/4$	$\delta t/8$	$\delta t/16$	$\delta t/32$
$\|\hat{u}_{h,\delta t} - u_{h,\delta t/2}\|_0$	9.599e-4	2.676e-4	7.032e-5	1.800e-5	4.553e-6	1.145e-6
Rate	/	1.84	1.93	1.97	1.98	1.99

(a)

Time step	$\delta t = 10^{-3}$	$\delta t/2$	$\delta t/4$	$\delta t/8$	$\delta t/16$	$\delta t/32$
$\|\hat{u}_{h,\delta t} - u_{h,\delta t/2}\|_0$	3.238e-3	9.261e-4	2.449e-4	6.276e-5	1.587e-5	3.991e-6
Rate	/	1.87	1.92	1.96	1.98	1.99

(b)

Table 2: Numerical results for the spatial discretization for the 2D Allen-Cahn equation with (a) $S = 0$ and (b) S=1; the time step size is chosen sufficiently small.

Mesh	$h = 2\pi/8$	$h = 2\pi/16$	$h = 2\pi/32$	$h = 2\pi/64$	$h = 2\pi/128$
$\|u_{h,\delta t} - u_{h/2,\delta t}\|_0$	4.208e-2	1.094e-2	2.761e-3	6.918e-4	1.731e-4
Rate	/	1.94	1.99	2.00	2.00

(a)

Mesh	$h = 2\pi/8$	$h = 2\pi/16$	$h = 2\pi/32$	$h = 2\pi/64$	$h = 2\pi/128$
$\|u_{h,\delta t} - u_{h/2,\delta t}\|_0$	4.208e-2	1.094e-2	2.760e-3	6.918e-4	1.730e-4
Rate	/	1.94	1.99	2.00	2.00

(b)

Fig. 1(a) shows the energy evolution of the 2D Allen-Cahn equation on using three different step sizes for $S = 0$ and $t \in [0, 0.5]$ — i.e. the standard CN/AB time discretization is employed. Obviously, with $\delta t = 0.01$ the resulting energy curve is bounded but not decreasing. One side effect is that the corresponding solution contour indicates that the maximum values exceed the theoretical maximum values in quite large areas — cf. Fig. 1(b). With a smaller time step size $\delta t = 0.005$, the energy curve is decreasing but the maximum norm of the numerical solution is slightly greater than 1 in a small portion of the solution domain — cf. Fig. 1(c). With a very small time step size $\delta t = 0.001$, the

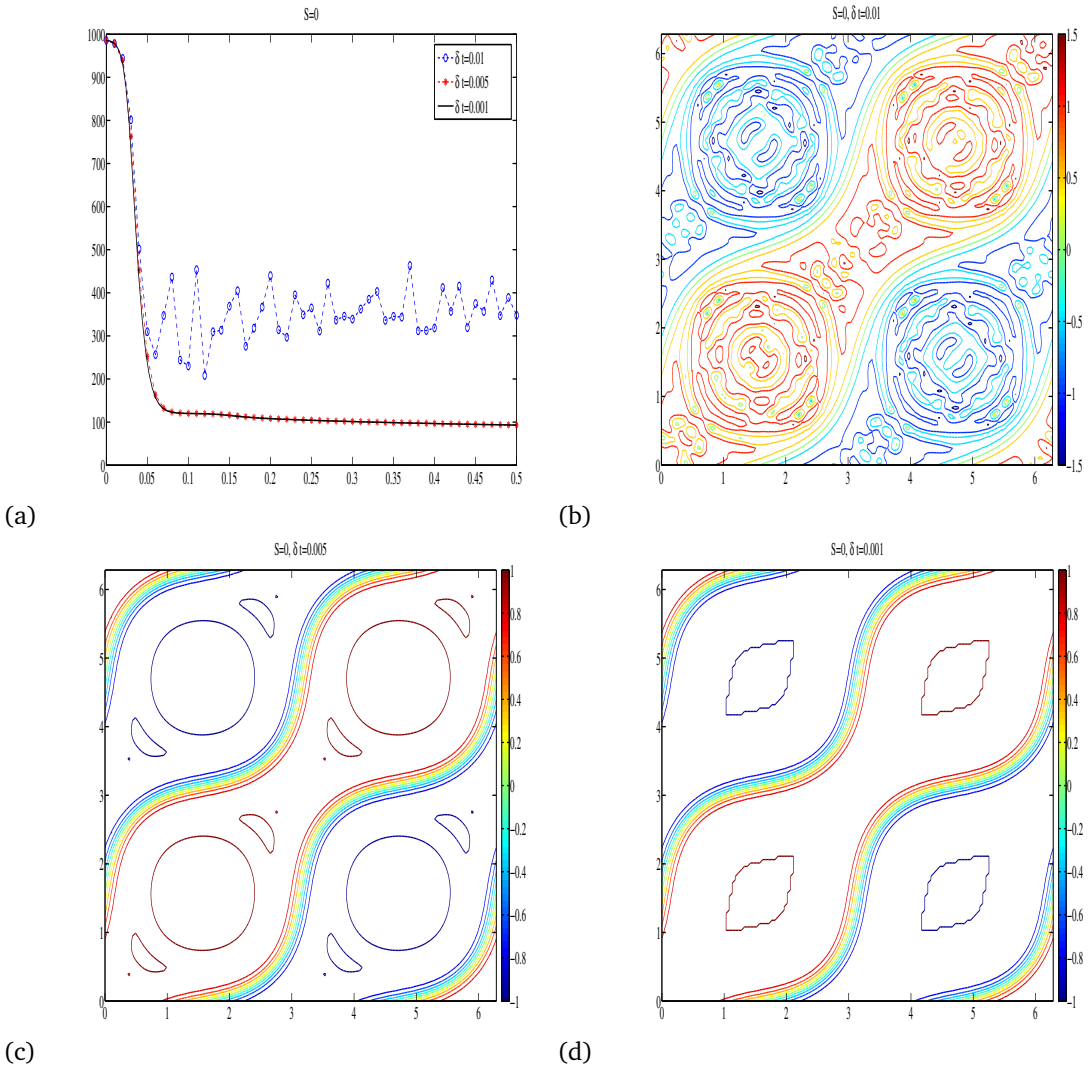

Figure 1: (a) The energy evolution for the 2D Allen-Cahn equation for $S = 0, t \in [0, 0.5]$; and the contour lines at $T = 0.5$ for (b) $\delta t = 0.01$, (c) $\delta t = 0.005$, and (d) $\delta t = 0.001$.

energy curve is decreasing and the maximum norm of the numerical solution is not greater than 1 in the entire solution domain — cf. Fig. 1(d).

Fig. 2(a) shows the energy evolution of the 2D Allen-Cahn equation on using three different time steps for $S = 1$. As shown in Fig. 2(b), when $\delta t = 0.01$ the energy is bounded but the maximum principle is not preserved. By adding a stabilization term in Algorithm 3.1, the properties of the numerical solutions with $\delta t = 0.005$ and $\delta t = 0.001$ are improved — cf. Figs. 2(c) and (d).

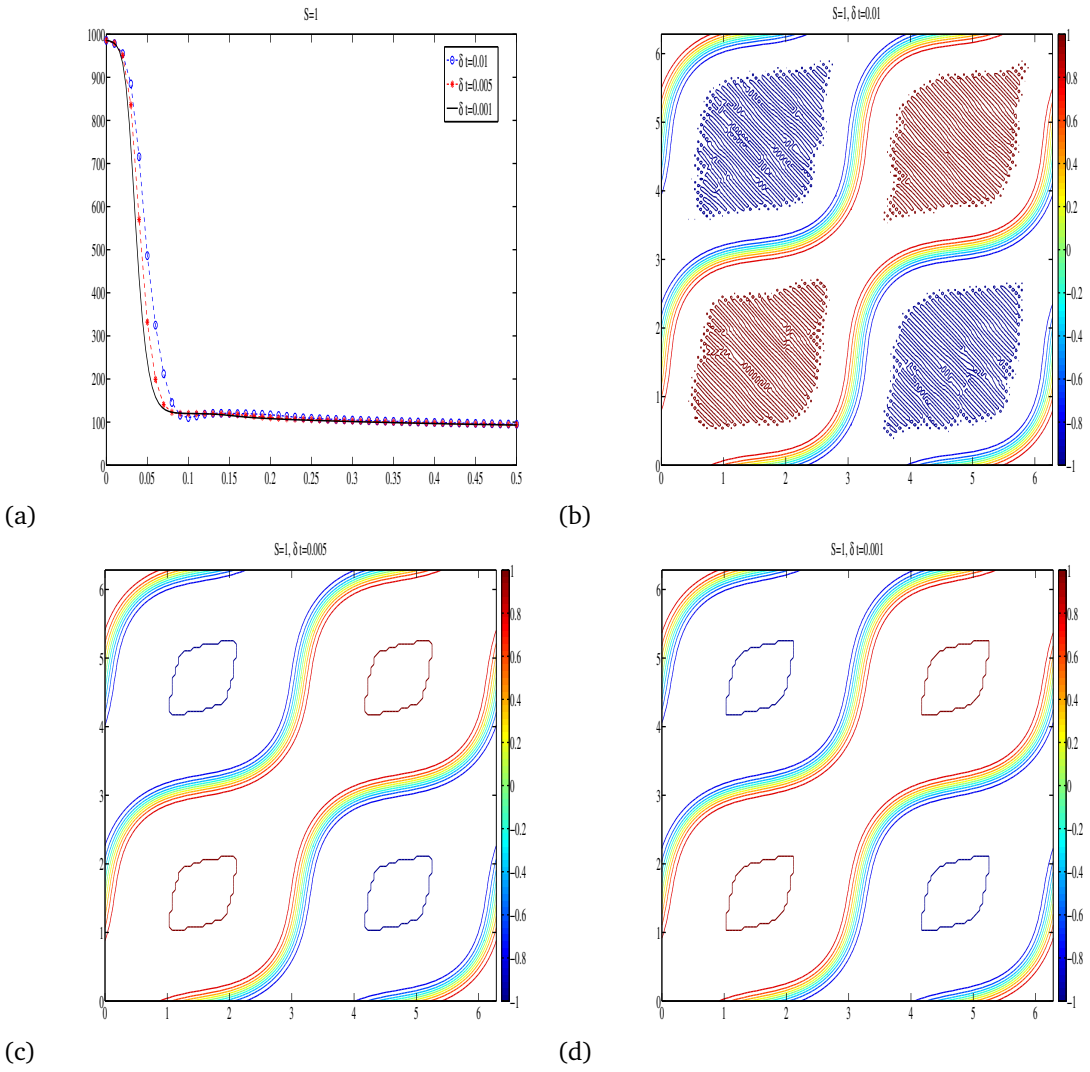

Figure 2: Same display as in Fig. 1, except that $S = 1$ (i.e. a stabilization term is added).

4.2. 2D Cahn-Hilliard equation

For the 2D Cahn-Hilliard equation, the initial condition is taken to be the small amplitude trigonometric function

$$u_0(x,y) = 0.1(\sin(3x)\sin(2y) + \sin(5x)\sin(5y)).$$

We again adopt a periodic boundary condition, the parameter $\epsilon = 0.1$, and $\Omega = [0, 2\pi] \times [0, 2\pi]$ for the solution domain.

The procedure is similar to that in the last subsection. The numerical results are first obtained on P_1-conforming element and the spatial step $h = 2\pi/128$. Table 3 shows the

Table 3: Numerical results for the time discretization for the 2D Cahn-Hilliard equation with (a) $S = 0$ and (b) $S = 1$.

Time step	$\delta t = 10^{-6}$	$\delta t/2$	$\delta t/4$	$\delta t/8$	$\delta t/16$
$\|u_{h,\delta t} - u_{h/2,\delta t}\|_0$	1.750e-7	4.558e-8	1.163e-8	2.935e-9	7.373e-10
Rate	/	1.94	1.97	1.99	1.99
$\|w_{h,\delta t} - w_{h/2,\delta t}\|_0$	1.145e-2	5.715e-3	2.855e-3	1.427e-3	7.132e-4
Rate	/	1.00	1.00	1.00	1.00

(a)

Time step	$\delta t = 10^{-6}$	$\delta t/2$	$\delta t/4$	$\delta t/8$	$\delta t/16$
$\|u_{h,\delta t} - u_{h/2,\delta t}\|_0$	4.139e-7	1.073e-7	2.731e-8	6.889e-9	1.730e-9
Rate	/	1.95	1.97	1.99	1.99
$\|w_{h,\delta t} - w_{h/2,\delta t}\|_0$	1.159e-2	5.746e-3	2.863e-3	1.430e-3	7.137e-4
Rate	/	1.01	1.01	1.00	1.00

(b)

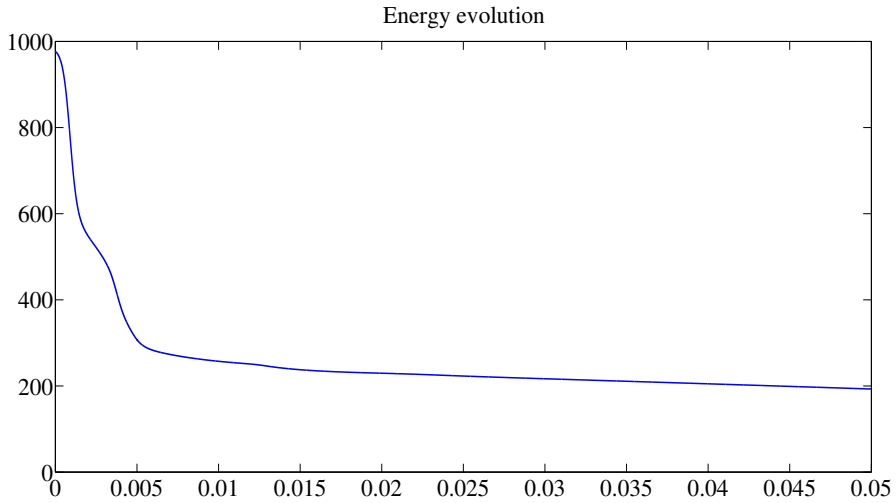

Figure 3: The energy evolution for the 2D Cahn-Hilliard equation with $S = 1$ and $t \in [0,\ 0.05]$.

L^2-errors obtained using various time step sizes, at $T = 10^{-4}$ (after 100 to 1600 time evolutions). The numerical scheme evidently gives optimal convergence rate in time — second-order convergence for u and first-order for w, respectively. Second-order spatial convergence similar to the last subsection was also observed, so that does not need to be discussed further here.

Finally, in Figs. 3 and 4 we plot the energy curve and solution contours obtained using $\delta t = 10^{-6}$. In both cases we used $S = 1$, with the stabilization terms added as in Algorithm 3.1. (When we used $S = 0$ with $\delta t = 10^{-6}$, we found that the numerical results “blow up" at the finite time $t = 0.01$, which is avoided on using the stabilized scheme.)

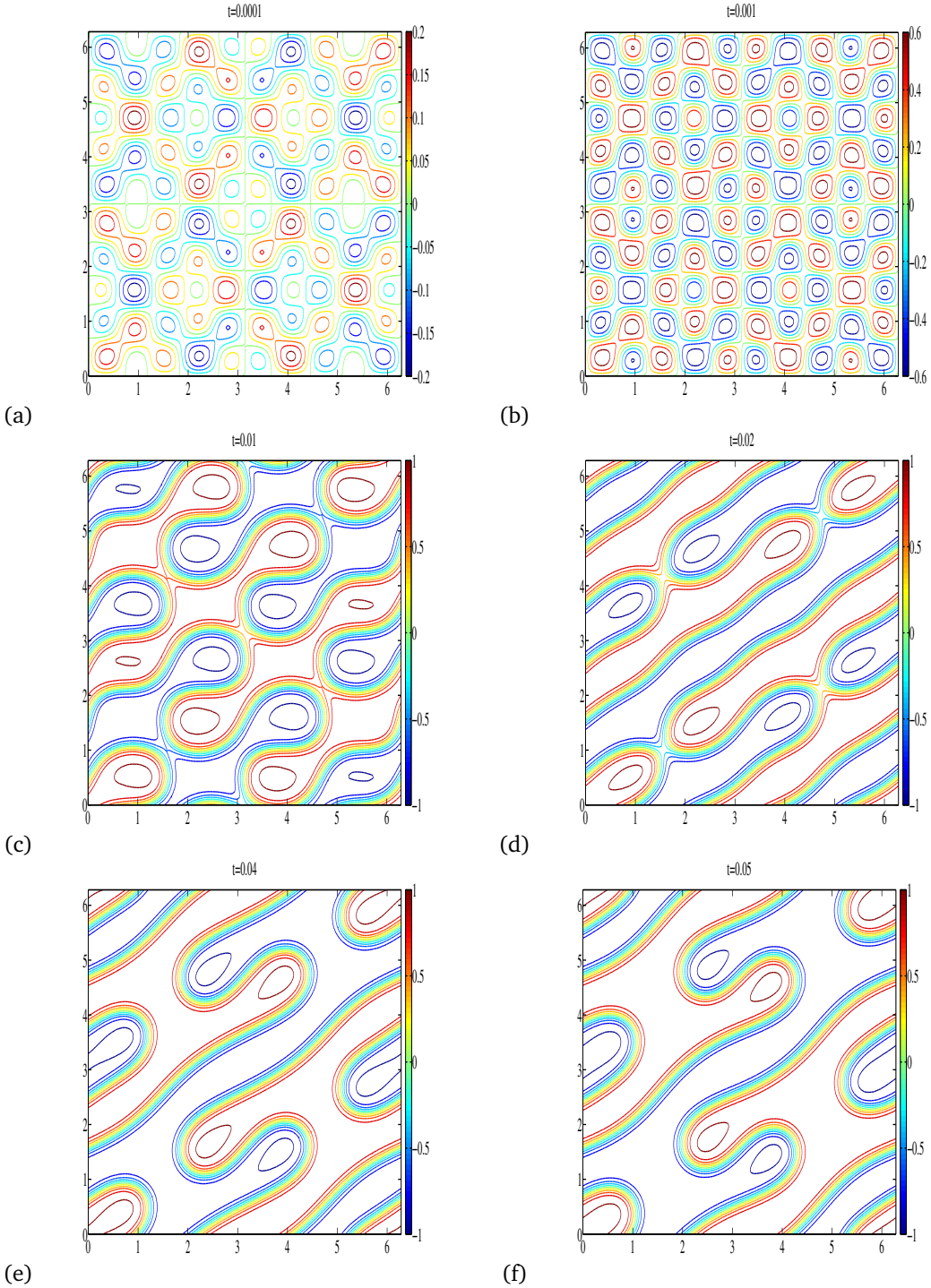

Figure 4: The time evolution of second-order scheme with $S = 1$ for the 2D Cahn-Hilliard example. Contour line at (a): $t = 10^{-4}$; (b): $t = 10^{-3}$; (c): $t = 10^{-2}$; (d): $t = 0.02$; (e): $t = 0.04$; and (f): $t = 0.05$.

We conclude this section by reporting a numerical observation — viz. that with the proposed stabilized schemes we can obtain satisfactory energy profiles for larger times of T. For example, we can extend the curve in Fig. 1 to $T = 5$, and the curve in Fig. 3 to $T = 0.5$. As the perturbation parameters in both (1.1) and (1.2) behave like ϵ^{-2}, the corresponding numerical solutions generally approach a steady state — as demonstrated in Fig. 1(a) and Fig. 3, after $t \approx O(10^{-1})$ for (1.1) and $t \approx O(10^{-2})$ for (1.2), respectively. Our computations can therefore cover the entire unsteady and steady time regimes.

5. Conclusions

In this article, we present a class of stabilized second-order Crank-Nicolson/Adams-Bashforth discretization with conforming finite element approximation for the nonstationary Allen-Cahn and Cahn-Hilliard equations. The resulting semi-discretized schemes are energy stable on choosing suitable stabilization parameters. The allowed time-step size to ensure energy stability can be larger compared with previously proposed schemes in Ref. [18]. For the fully discretized schemes, optimal error estimates are obtained. Numerical experiments are carried out to show the efficiency of the proposed scheme in solving the Allen-Cahn and Cahn-Hilliard equations.

These schemes can be extended to three dimensions quite easily — and it is also possible to extend the present schemes and analysis to other nonlinear phase field models, such as epitaxial growth models [14, 16, 21].

Acknowledgments

The first author is partially supported by the NSF of China (No. 11271313) and Hong Kong Scholars Program. The second and third authors are partially supported by Hong Kong Research Grant Council GIF grants and Hong Kong Baptist University FRG grants.

References

[1] S.M. Allen, J.W. Cahn, A microscopic theory for antiphase boundary motion and its application to antiphase domain coarsening, Acta Metall. 27 (1979) 1085-1095.

[2] Uri M. Ascher, J. Ruuth, R.J. Spiteri, Implicit-Explicit Runge-Kutta method for time dependent partial differential equations, Appl. Numer. Math. 25 (1997) 151-167.

[3] A.L. Bertozzi, N. Ju, H.-W. Lu, A biharmonic modified forward time stepping method for fourth order nonlinear diffusion equations, Discrete Contin. Dyn. Syst. 29(4) (2011) 1367-1391.

[4] A.L. Bertozzi, S. Esedoglu, A. Gillette, Analysis of a two-scale Cahn-Hilliard model for image inpainting, Multi. Model. Simul. 6(3) (2007) 913-936.

[5] A.L. Bertozzi, S. Esedoglu, A. Gillette, Inpainting of binary images using the Cahn-Hilliard equation, IEEE Trans. Image Proc. 16(1) (2007) 285-291.

[6] S. Boscarino, L. Pareschi, G. Russo, Implicit-Explicit Runge-Kutta schemes for hyperbolic systems and kinetic equations in the diffusion limit, SIAM J. Sci. Comp. to appear.

[7] J.W. Cahn, J.E. Hilliard, Free energy of a nonuniform system, I: Interfacial free energy, J. Chem. Phys. 28(2) (1958) 258-267 .
[8] Q. Du, R.A. Nicolaides, Numerical analysis of a continuum model of phase transition, SIAM J. Numer. Anal. 28 (1991) 1310-1322.
[9] D.J. Eyre, An unconditionally stable one-step scheme for gradient systems, unpublished, http://www.math.utah.edu/eyre/research/methods/stable.ps.
[10] X. Feng, H. Song, T. Tang, J. Yang, Nonlinearly stable implicit-explicit methods for the Allen-Cahn equation, Preprint.
[11] H. Gomez, T.J.R. Hughes, Provably unconditionally stable, second-order time-accurate, mixed variational methods for phase-field models, J. Comput. Phys. 230(13) (2011) 5310–5327.
[12] Y. He, Y. Liu, T. Tang, On large time-stepping methods for the Cahn-Hilliard equation, Appl. Numer. Math. 57 (2007) 616-628.
[13] Z. Hu, S.M. Wise, C. Wang, J.S. Lowengrub, Stable and efficient finite-diffence nonlinear multigrid schemes for the phase field crystal equation, J. Comput. Phys. 228 (2009) 5323-5339.
[14] B. Li, J.-G. Liu, Thin film epitaxy with or without slope selection, European J. Appl. Math. 14(6) (2003) 713-743.
[15] Z. Qiao, Z. Sun, Z. Zhang, The stability and convergence of two linearized finite difference schemes for the nonlinear epitaxial growth model, Numer. Methods Part. Diff. Eq. 28(6) (2012) 1893-1915.
[16] Z. Qiao, Z. Zhang, T. Tang, An adaptive time-stepping strategy for the molecular beam epitaxy models, SIAM J. Sci. Comput. 33 (2011) 1395-1414.
[17] J. Shen, T. Tang, L. Wang, Spectral Methods: Algorithms, Analysis and Applications, Volume 41 of Springer Series in Computational Mathematics, Springer, 2011.
[18] J. Shen, X. Yang, Numerical approximations of Allen-Cahn and Cahn-Hilliard equations, Discrete Contin. Dyn. Syst.-A 28 (2010) 1669-1691.
[19] J. Shen, X. Yang, A phase-field model and its numerical approximation for two-phase incompressible flows with different densities and viscosities, SIAM J. Sci. Comput. 32 (2010) 1159-1179.
[20] S.M. Wise, C. Wang, J.S. Lowengrub, An energy stable and convergent finite difference scheme for the phase field crystal equation, SIAM J. Numer. Anal. 47 (2009) 2269-2288.
[21] C. Xu, T. Tang, Stability analysis of large time-stepping methods for epitaxial growth models, SIAM J. Numer. Anal. 44 (2006) 1759-1779.
[22] X. Yang, Error analysis of stabilized semi-implicit method of Allen-Cahn equation, Discrete Contin. Dyn. Syst.-B 11 (2009) 1057-1070.
[23] J. Zhang, Q. Du, Numerical studies of discrete approximations to the Allen-Cahn equation in the sharp interface limit, SIAM J. Sci. Comput. 31(4) (2009) 3042-3063.
[24] Z. Zhang, Z. Qiao, An adaptive time-stepping strategy for the Cahn-Hilliard equation, Commun. Comput. Phys. 11 (2012) 1261-1278.